

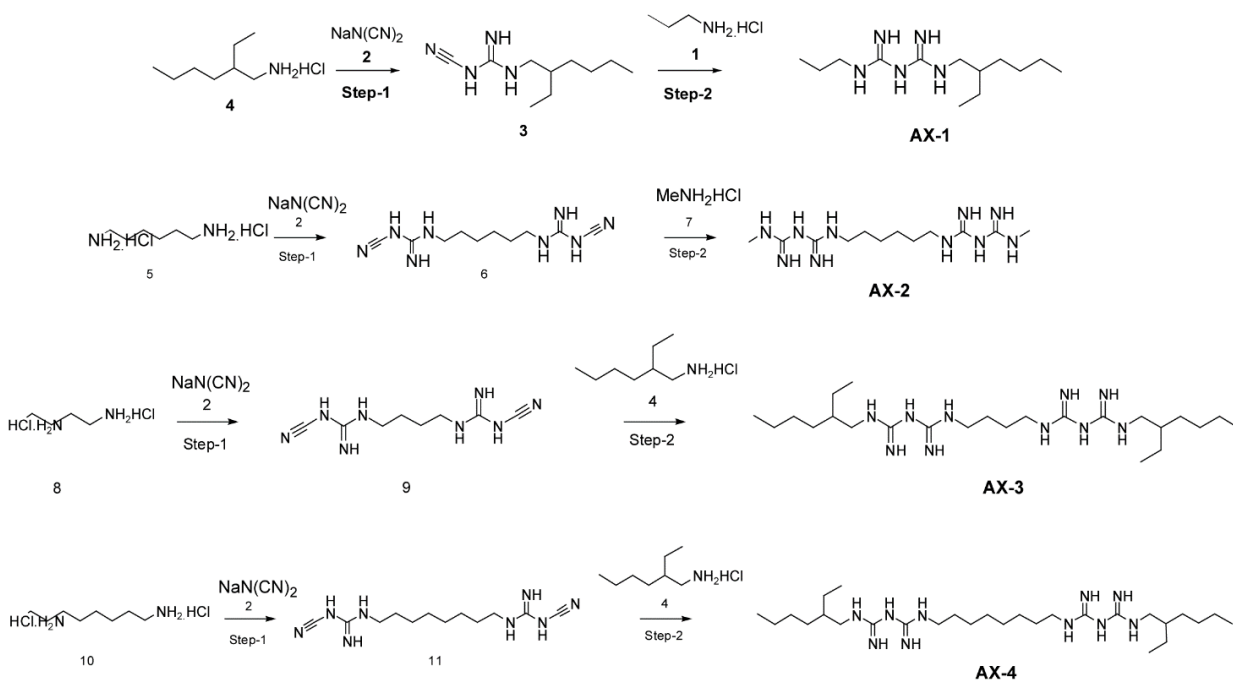
Supplemental information

**Bisbiguanide analogs induce
mitochondrial stress to inhibit
lung cancer cell invasion**

Christina M. Knippler, Jamie L. Arnst, Isaac E. Robinson, Veronika Matsuk, Tala O. Khatib, R. Donald Harvey, Mala Shanmugam, Janna K. Mouw, Haiyan Fu, Thota Ganesh, and Adam I. Marcus

Supplemental Information

A



B

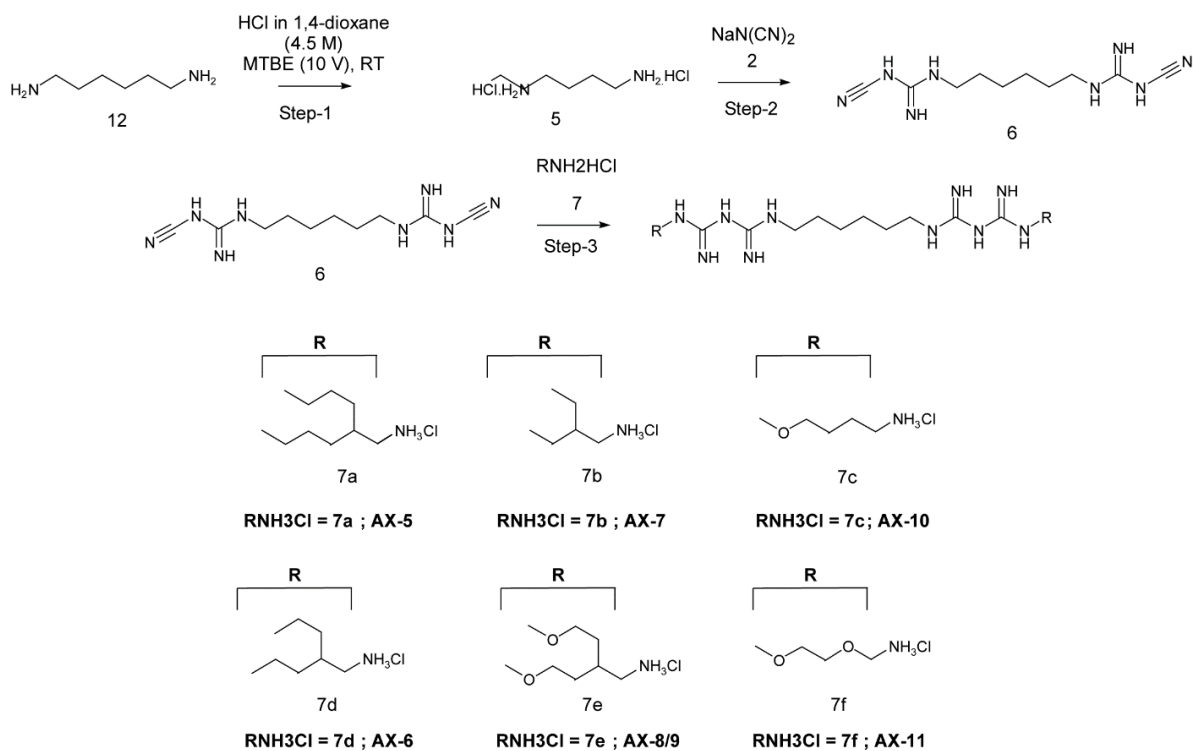


Figure S1. Reaction schemes for the alexidine analogs related to Figure 1 and STAR methods. (A) Reaction schemes for AX-1, AX-2, AX-3, and AX-4. (B) Reaction schemes for AX-5, AX-7, and AX-10. Intermediate reactions were the same for AX-5, AX-7, and AX-10. The R structure for compound **7** in the final step (Step-3) is shown for each analog below (i.e. **7a**, **7b**, and **7c**). AX-6, AX-8/9, and AX-11 were unable to be synthesized, but structure design is shown (i.e. **7d**, **7e**, and **7f**).

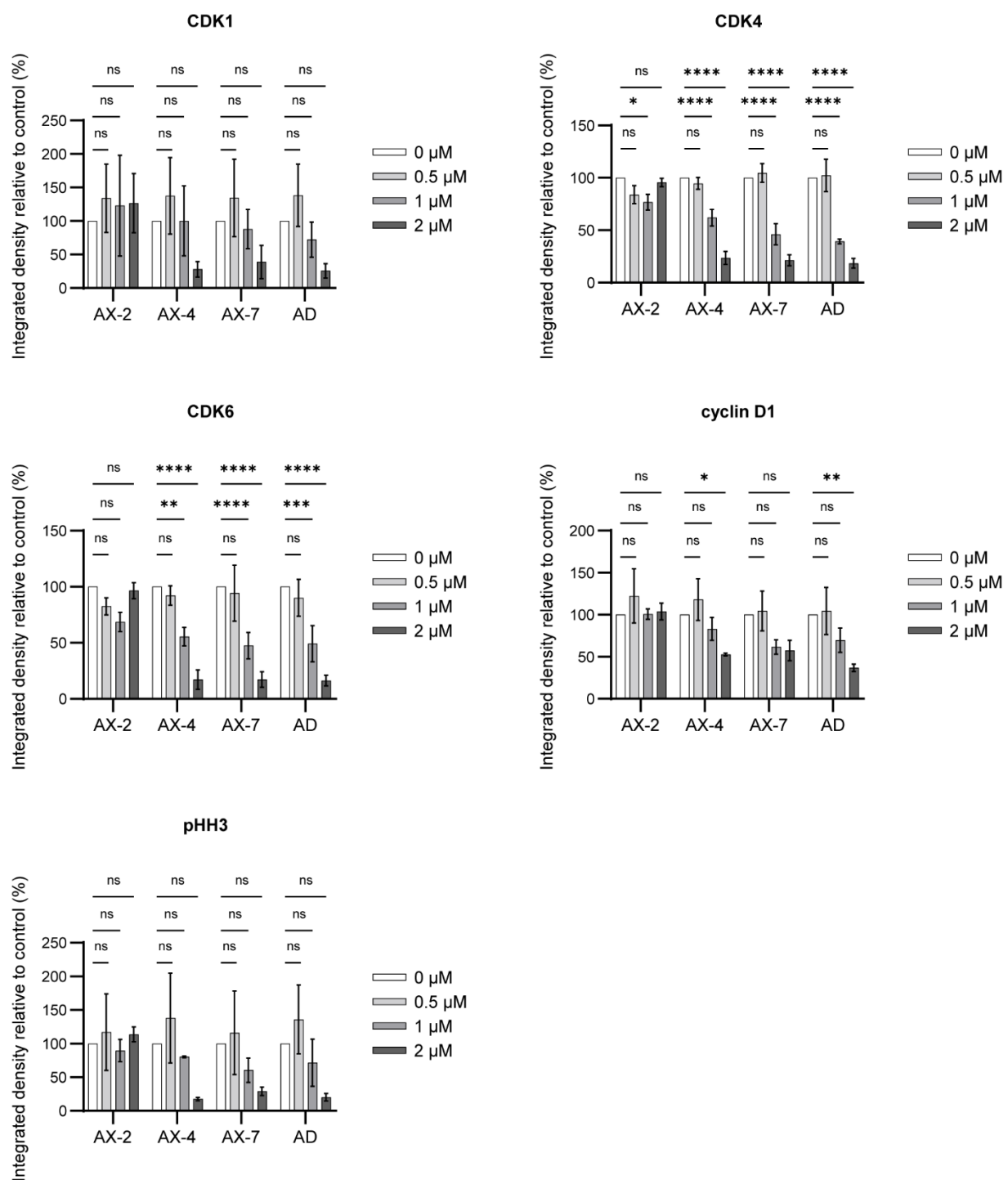


Figure S2. Quantification of cell cycle-related proteins as detected by western blot, related to Figure 1 for representative western blots. Data are normalized to actin and relative to the DMSO control. Mean \pm SD is shown of three biological replicates. Significance was assessed using an ordinary two-way ANOVA with a Tukey's multiple comparisons test, * $p \leq 0.05$, ** $p \leq 0.01$, *** $p \leq 0.001$, **** $p \leq 0.0001$

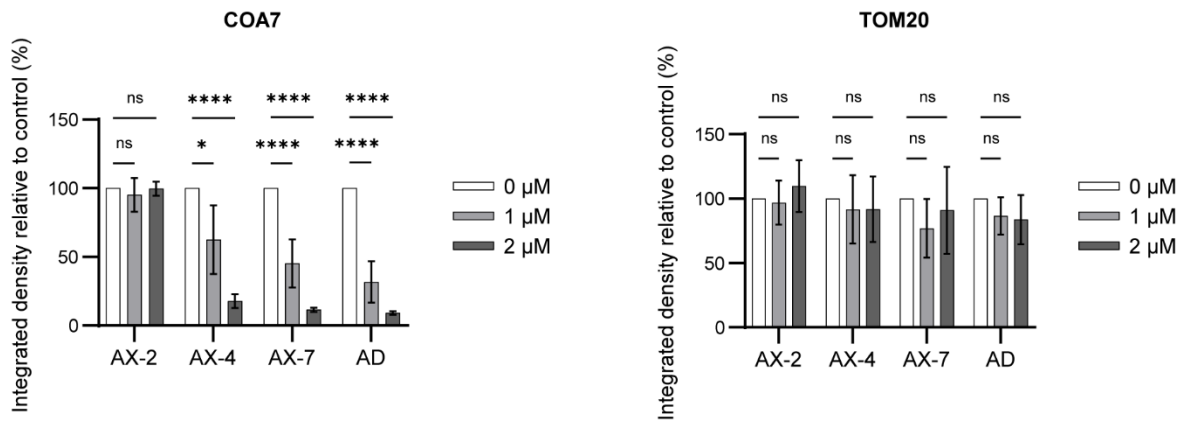


Figure S3. Quantification of mitochondria-related proteins as detected by western blot, related to Figure 3 for representative western blots. Data are normalized to actin and relative to the DMSO control. Mean \pm SD is shown of three biological replicates. Significance was assessed using an ordinary two-way ANOVA with a Tukey's multiple comparisons test, * $p \leq 0.05$, ** $p \leq 0.01$, *** $p \leq 0.001$, **** $p \leq 0.0001$

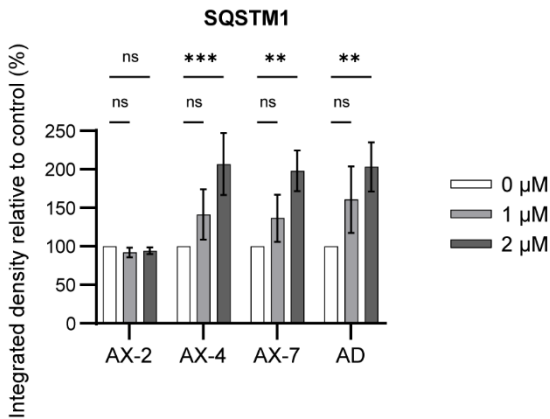


Figure S4. Quantification of SQSTM1 as detected by western blot, related to Figure 4 for representative western blots. Data are normalized to actin and relative to the DMSO control. Mean \pm SD is shown of three biological replicates. Significance was assessed using an ordinary two-way ANOVA with a Tukey's multiple comparisons test, * $p \leq 0.05$, ** $p \leq 0.01$, *** $p \leq 0.001$, **** $p \leq 0.0001$

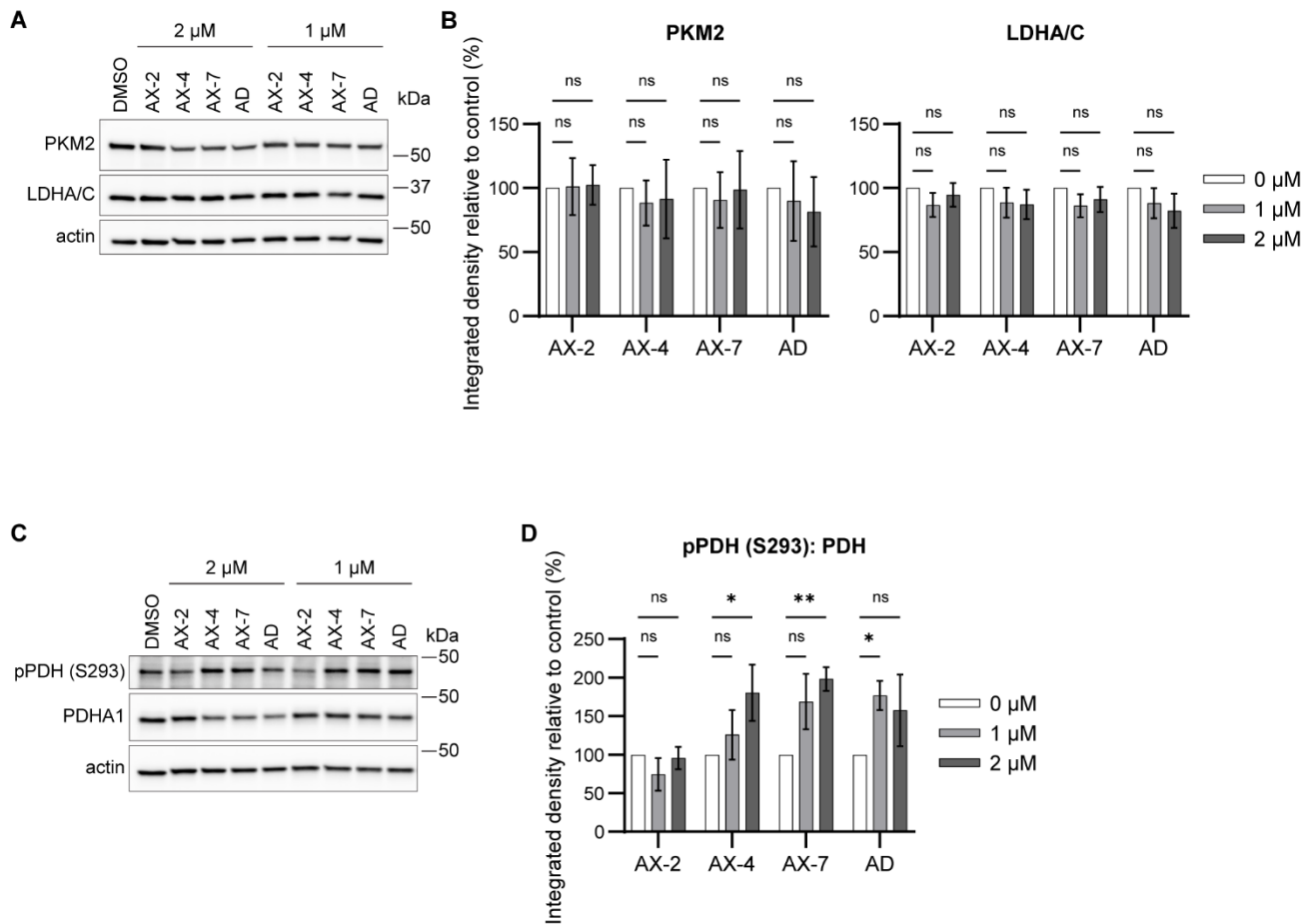


Figure S5. Alexidine analogs shift metabolism towards glycolysis, related to Figure 4. H1299 cells were treated for 48 hr with the analogs as indicated. Lysates were separated by western blot and probed for (A) pyruvate kinase M2 (PKM2), lactate dehydrogenase A/C (LDHA/C) and (C) pyruvate dehydrogenase (PDHA1) and phosphorylated PDH at serine 293 (pPDH (S293)). (B) Quantification of PKM2 and LDHA/C western blots are normalized to actin and relative to the DMSO control. (C) Quantification of the ratio of pPDH (S293) and total PDHA1 relative to DMSO control. Mean \pm SD is shown of three biological replicates. Significance was assessed using an ordinary two-way ANOVA with a Tukey's multiple comparisons test, * $p \leq 0.05$, ** $p \leq 0.01$, *** $p \leq 0.001$, **** $p \leq 0.0001$

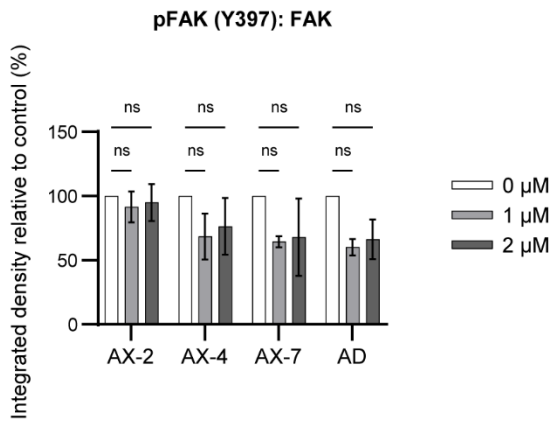


Figure S6. Quantification of the ratio of phosphorylated FAK (pFAK (Y397)) and total FAK as detected by western blot, related to Figure 5 for representative western blots. Data are normalized relative to the DMSO control. Mean \pm SD is shown of three biological replicates. Significance was assessed using an ordinary two-way ANOVA with a Tukey's multiple comparisons test, * $p \leq 0.05$, ** $p \leq 0.01$, *** $p \leq 0.001$, **** $p \leq 0.0001$

Table S1. Permeability of Analogs in Caco-2 Cells					
Compound	$P_{app(A-B)}$ (10^{-6} , cm/s)	$P_{app(B-A)}$ (10^{-6} , cm/s)	Efflux Ratio	Recovery (%) AP-BL	Recovery (%) BL-AP
Propranolol	18.45	13.20	0.72	66.75	75.16
Digoxin	0.27	13.68	50.72	87.02	83.49
Alexidine	<0.07	0.37	>5.37	<24.36	28.15
AX-1	<0.03	6.74	>236.12	<57.15	66.57
AX-2	0.62	0.37	0.60	66.25	87.87
AX-4	<0.04	0.30	>6.88	<22.28	24.32
AX-7	0.27	0.53	1.95	81.30	75.30

Table S1. Permeability of Analogs in Caco-2 Cells, related to Figure 2. P_{app} = apparent permeability; A, AP= apical; B, BL= basolateral

Table S2. Assessment of Caco-2 Monolayer Integrity				
Compound	TEER _{A-B} ($\Omega \times \text{cm}^2$)	TEER _{B-A} ($\Omega \times \text{cm}^2$)	LY Leakage _{A-B} (%)	LY Leakage _{B-A} (%)
Propranolol	318	342	0.23	0.21
Digoxin	504	453	0.18	0.15
Alexidine	477	496	0.16	0.15
AX-1	490	507	0.14	0.15
AX-2	504	507	0.15	0.13
AX-4	508	490	0.16	0.15
AX-7	444	494	0.18	0.11

Table S2. Assessment of Caco-2 Monolayer Integrity, related to Figure 2. TEER= transepithelial electrical resistance; A= apical; B= basolateral; LY= Lucifer Yellow

Compound	Species	<i>In vitro</i> T _{1/2} (min)	<i>In vitro</i> Cl _{int} (μL/min/mg protein)	Scale-up Cl _{int} (mL/min/kg)
Verapamil	Human	18.17	76.29	95.69
	Monkey	3.22	430.31	645.46
	Dog	19.35	71.62	178.52
	Rat	7.38	187.76	336.47
	Mouse	10.32	134.25	590.70
7-OH coumarin	Human	1.85	748.86	939.19
	Monkey	2.45	564.73	847.09
	Dog	2.01	691.09	1722.76
	Rat	2.42	573.25	1027.26
	Mouse	2.00	692.10	3045.24
AX-7	Human	668.14	2.07	2.60
	Monkey	84.51	16.40	24.60
	Dog	1888.13	0.73	1.83
	Rat	36.61	37.86	67.85
	Mouse	64.63	21.44	94.35

Table S3. Metabolic Stability of AX-7 in Different Species of Liver Microsomes, related to Figure 2. T_{1/2}= half-life; Cl_{int}= intrinsic clearance. Scale-up uses scaling factors based on the species' liver weight, microsomal concentration, and liver blood flow to estimate *in vivo* clearance.

Compound	Species	<i>In vitro</i> T _{1/2} (min)	<i>In vitro</i> Cl _{int} (μL/min/10 ⁶ cells)	Scale-up Cl _{int} (mL/min/kg)
Verapamil	Human	26.14	53.02	134.89
	Monkey	10.00	138.64	499.09
	Dog	32.24	42.99	295.79
	Rat	20.00	69.30	324.32
	Mouse	16.43	84.36	996.52
AX-7	Human	∞	0.00	0.00
	Monkey	168.57	8.22	29.60
	Dog	151.80	9.13	62.82
	Rat	129.01	10.74	50.28
	Mouse	129.48	10.70	126.45

Table S4. Metabolic Stability of AX-7 in Different Species of Hepatocytes, related to Figure 2. T_{1/2}= half-life; Cl_{int}= intrinsic clearance. If Cl_{int} < 0, then T_{1/2} and Cl_{int} were reported as "∞" and "0.00", respectively. Scale-up uses scaling factors based on the species' liver weight and hepatocyte concentration to estimate *in vivo* clearance.

Animal ID	Total AX-7 in Urine (ng)	Total AX-7 Administered (ng)	Excretory Rate (%)	Mean Excretory Rate (%)
A	5.94	51200	0.0116	0.017
B	11.4	50200	0.0228	
C	8.88	53200	0.0167	

Table S5. Excretory Rate in Urine of AX-7, related to Figure 2. Urine was collected within 4 hours of the last dose administered. AX-7 amount in the urine was detected by mass spectrometry and the excretory rate for each animal was calculated by dividing the amount of AX-7 in the urine by the amount administered via intraperitoneal injection.

Table S6: Proteins upregulated in Control vs. Alexidine: GO Biological Process		
Process Name	Fold Enrichment	False Discovery Rate (FDR)
positive regulation of chromosome condensation (GO:1905821)	35.75	3.36E-02
positive regulation of mitotic metaphase/anaphase transition (GO:0045842)	31.78	6.10E-04
anaphase-promoting complex-dependent catabolic process (GO:0031145)	16.58	3.31E-02
cholesterol biosynthetic process (GO:0006695)	15.46	1.67E-03
regulation of ubiquitin protein ligase activity (GO:1904666)	14.67	4.52E-02
mitotic spindle assembly (GO:0090307)	9.73	4.40E-02
mitotic metaphase plate congression (GO:0007080)	9.35	4.99E-02
regulation of muscle cell apoptotic process (GO:0010660)	8.67	2.35E-02
mitochondrial translation (GO:0032543)	6.12	4.00E-02
regulation of cold-induced thermogenesis (GO:0120161)	5.08	4.49E-02
cell division (GO:0051301)	4.57	9.85E-07
cellular component disassembly (GO:0022411)	3.52	4.15E-02
peptidyl-amino acid modification (GO:0018193)	2.73	1.07E-02
protein-containing complex assembly (GO:0065003)	2.13	3.44E-02

Table S6. Proteomics analyses of proteins upregulated in Control vs. Alexidine treated cells, related to Figure 1 and Figure 3. H1299 cells were treated for 48 hrs with DMSO (control) or 1 μ M alexidine. Proteins were isolated and assessed by mass spectrometry. Proteins with intensities that were at least two-fold higher in control cells than alexidine-treated cells were assessed by Gene Ontology (GO) and PANTHER using the GO Biological Process annotation data set. See all proteins detected in Table S8 (Excel file).

Table S7: Proteins upregulated in Control vs. Alexidine: GO Cellular Component		
Component Name	Fold Enrichment	False Discovery Rate (FDR)
ribonucleoside-diphosphate reductase complex (GO:0005971)	63.56	4.25E-02
centralspindlin complex (GO:0097149)	63.56	4.16E-02
condensin complex (GO:0000796)	35.75	9.16E-03
outer kinetochore (GO:0000940)	20.43	2.97E-02
anaphase-promoting complex (GO:0005680)	17.33	7.99E-03
mitochondrial small ribosomal subunit (GO:0005763)	11.92	2.36E-02
spindle pole (GO:0000922)	5.54	1.69E-03
mitochondrial inner membrane (GO:0005743)	2.88	1.52E-02
microtubule organizing center (GO:0005815)	2.24	3.65E-02
nucleoplasm (GO:0005654)	1.64	1.07E-03

Table S7. Proteomics analyses of proteins upregulated in Control vs. Alexidine treated cells, related to Figure 1 and Figure 3. H1299 cells were treated for 48 hrs with DMSO (control) or 1 μ M alexidine. Proteins were isolated and assessed by mass spectrometry. Proteins with intensities that were at least two-fold higher in control cells than alexidine-treated cells were assessed by Gene Ontology (GO) and PANTHER using the GO Cellular Component annotation data set. See all proteins detected in Table S8 (Excel file).